

A New Perspective on the Synchronverter Model

Georgios C. Kryonidis, *Member, IEEE*, Kyriaki-Nefeli D. Malamaki,
Juan Manuel Mauricio, *Senior Member, IEEE*, and Charis C. Demoulias

Abstract—In this short communication, a modified version of the well-established synchronverter model is proposed, introducing improved control characteristics that allow the efficient integration of converter-interfaced renewable energy sources to the electrical grid. In the proposed model, the inertial response is decoupled from the primary frequency response. Furthermore, a condition for a critically damped provision of inertial response is proposed. The improved performance of the proposed model against the variants of the synchronverter model is assessed by performing time-domain simulations and stability analysis.

Index Terms—Inertial response, primary frequency response, synchronverter.

I. INTRODUCTION

THE gradual replacement of large-scale conventional power plants with converter-interfaced renewable energy sources (CI-RESs) has brought new challenges to the electrical grid. Among them, the reduction of system inertia is considered as one of the most important issues affecting the secure and reliable grid operation [1]. A promising solution to this problem is to develop new control algorithms for the provision of virtual inertial response by CI-RESs. To this end, the authors in [2] proposed an innovative solution known as synchronverter, where CI-RESs are properly controlled to imitate the behavior of synchronous generators.

An inherent drawback of the synchronverter model is the poor damping of oscillations which is inconsistent with the requirements posed by the European network of transmission system operators for electricity (ENTSO-E) [3] and may jeopardize the dynamic stability of the grid. In the literature, this issue can be addressed either at power system level or at model level. In the first case, the model parameters are adapted to the varying operating conditions of the grid. In particular, the authors in [4] propose a rule-based control scheme to adjust the inertia and damping constants of the model. A similar approach has been recently proposed by the authors in [5], [6], where a linear quadratic regulator-based optimization technique is used to adaptively adjust the inertia and damping constants according to the frequency disturbance. Although these methods are valid and can effectively damp oscillations at power system level, the inherent drawback of the synchronverter model, i.e., poor damping of oscillations at model level, still persists.

In the second case, the initial structure of the synchronverter model is modified to improve its dynamic stability. More specifically, the authors in [7] introduce five modifications

including the virtual inductor, virtual capacitor, and anti-windup mechanisms. The latter is employed to improve the stability of the model under abnormal conditions by limiting the field current. A similar approach is proposed in [8] where the conventional integral controller is replaced by a second-order system providing boundaries to the controlled variables, i.e., the local angular frequency and the field current. Nevertheless, both solutions overlook the inherent oscillatory dynamic behavior of the synchronverter model. This issue is partially addressed in [9] by proposing an improved damping method. However, the damping is introduced in the magnitude of the internal voltage of the model which strongly affects the reactive power output. An alternative solution involves the use of a phase-locked loop (PLL) [10], which, however, increases the complexity of the model.

Apart from the poor damping of oscillations, the inertial response (IR) is coupled with the primary frequency response (PFR) in all the afore-mentioned studies, hindering the distinct handling of these functionalities. As a result, an additional burden is placed towards the accurate measurement, and thus remuneration, of these functionalities to be treated as ancillary services (ASs).

In this paper, a new structure of the synchronverter model is proposed. The proposed model is characterized by improved damping of oscillations and the effective decoupling of IR and PFR. Moreover, the active and reactive power loops are fully decoupled in the proposed model. Finally, a closed-form expression for a critically damped IR provision is proposed being also in line with the requirements posed by ENTSO-E. Contrary to the use of typical frequency variation curves [5], the performance of the proposed model is evaluated under a frequency ramp variation to clearly demonstrate the difference between IR and PFR.

II. PROPOSED MODEL

The control logic of the proposed model is presented in Fig. 1 consisting of two parallel control loops, namely the active (APCL) and the reactive power control loop (RPCL). APCL aims at controlling the output active power (P) of the CI-RES by modifying the angle (θ) of the internal voltage. This is attained by introducing a proportional-integral (PI) controller as follows:

$$\ddot{\theta} = k_i^f (P_s - P) - \underbrace{k_p^f \dot{P}}_{\text{damping term}} \quad (1)$$

where $\ddot{\theta}$ denotes the second derivative of θ , P_s is the reference active power, and \dot{P} is the first derivative of P . Furthermore, k_p^f and k_i^f are the coefficients of the proportional and integral terms of the PI controller, respectively. The former provides damping to the dynamic performance of the model, while the

This work is part of and supported by the European Union, Horizon 2020 project "EASY-RES" with Grant agreement: 764090.

G. C. Kryonidis, K.-N. D. Malamaki, and C. S. Demoulias are with the School of Electrical and Computer Engineering, Aristotle University of Thessaloniki, Thessaloniki GR 54124, Greece (e-mail: kryonidi@ece.auth.gr; nmalamak@ece.auth.gr; chdimoul@auth.gr).

J. M. Mauricio is with the Department of Electrical Engineering, Universidad de Sevilla, 41092 Sevilla, Spain (e-mail: j.m.mauricio@ieec.org).

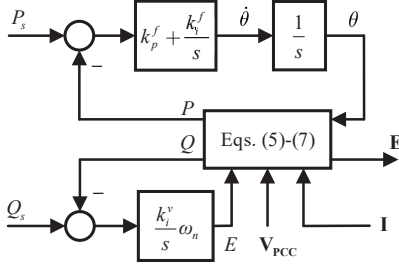


Fig. 1. Control logic of the proposed model.

latter is associated with the IR provision and can be determined by the inertia constant (H) using (2).

$$k_i^f = \frac{1}{2H} \quad (2)$$

The APCL is modeled in the synchronverter as follows:

$$\ddot{\theta} = k_i^f \left(P_s - P - \underbrace{D_p(\omega - \omega_n)}_{\text{damping term}} \right) \quad (3)$$

where ω and ω_n are the angular frequency of the internal voltage ($\dot{\theta}$) and the nominal angular frequency, respectively. According to (3), it can be observed that the damping term indirectly introduces the PFR functionality in the synchronverter since it is proportional to the difference between ω and ω_n . As a result, the IR is always coupled with the PFR in the synchronverter model since the latter is necessary for damping oscillations. Note that an increase of the damping coefficient (D_p) will improve the dynamic behavior of the model at the expense of increased PFR provision. This issue is addressed in the proposed model by introducing a new damping scheme via the use of a PI controller as shown in (1).

Scope of the RPCL is to control the output reactive power (Q) of the CI-RES by modifying the magnitude (E) of the internal voltage using an integral controller as follows:

$$\dot{E} = k_i^v \omega_n (Q_s - Q) \quad (4)$$

where \dot{E} stands for the first derivative of E , Q_s is the reference reactive power, and k_i^v is the coefficient of the integral controller.

The output active and reactive power of the CI-RES are calculated using (5) and (6).

$$P = \mathbf{V}_{PCC}^T \mathbf{I} \quad (5)$$

$$Q = \mathbf{V}_{PCC}^T (\mathbf{A} - \mathbf{B}) \mathbf{I} \quad (6)$$

\mathbf{V}_{PCC} and \mathbf{I} are 3×1 vectors containing the phase-to-neutral voltages at the point of common coupling (PCC) and output currents, respectively. Moreover, \mathbf{A} and \mathbf{B} stand for the auxiliary 3×3 shift matrices. These are binary matrices where the elements are calculated using the Kronecker delta. More specifically, $A = \delta_{i+2,j} + \delta_{i,j+1}$ and $B = \delta_{i+1,j} + \delta_{i,j+2}$. By combining the outputs of both control loops, the reference internal voltage of the CI-RES is determined using (7).

$$\mathbf{E} = E \sin \Theta \quad (7)$$

Here, \mathbf{E} and Θ are 3×1 vectors containing the phase-to-neutral reference voltages and the corresponding voltage angles. It

is worth mentioning that the voltage angle of phase a is calculated using (1), while the angles of the phases b and c are determined by subtracting $2\pi/3$ and $4\pi/3$ from the voltage angle of phase a , respectively.

III. CONDITION FOR CRITICALLY DAMPED SYSTEM

Scope of this section is to provide a condition for a critically damped system. Assuming the reactance of the output LC filter of the CI-RES is X_c , the output active power is calculated as follows:

$$P = \frac{3EV_{PCC}}{2X_c} \sin \delta \quad (8)$$

where δ is the angle difference between the internal voltage and the PCC voltage. Since CI-RESs are characterized by a relatively small reactance, the operating values of δ will be very small and the following approximations can be considered: $\sin \delta \approx \delta$ and $\cos \delta \approx 1$. By substituting (8) to (1), (9) is obtained.

$$\dot{\omega} = -k_i^f \left(P_s - \frac{3EV_{PCC}}{2X_c} \delta \right) - \underbrace{k_p^f \frac{3EV_{PCC}}{2X_c} (\omega - \omega_g)}_{\text{damping term}} \quad (9)$$

By contrasting (3) with (9), the main difference in modelling the damping term can be observed. In particular, ω_n in the synchronverter model is replaced by ω_g in the proposed model which is the angular frequency of the grid. Therefore, PFR is absent during IR provision since any dependence of the damping term on the deviation of ω from ω_n is removed. As a result, PFR can be independently controlled in the proposed model by simply modifying the active power reference P_s . Note that in (9), ω_g is not measured via a PLL as proposed in [10] but it is indirectly included in the calculation of the output active power. By differentiating (9) and applying Laplace transformation, (10) is derived.

$$\frac{P}{\Omega_g} = -\frac{s}{\frac{2X_c}{3EV_{PCC}} s^2 + k_p^f s + k_i^f} \quad (10)$$

To ensure a critically damped system, the determinant of the denominator in (10) should be equal to zero, leading to (11).

$$k_p^{f2} = \frac{8X_c}{3EV_{PCC}} k_i^f \quad (11)$$

It is evident that k_p^f is calculated with respect to known parameters, i.e., the voltage magnitudes of the internal voltage and PCC voltage, the filter reactance X_c , and k_i^f which is determined according to (2).

IV. PRIMARY FREQUENCY RESPONSE

The mathematical formulation of the PFR is presented below:

$$P_s = \begin{cases} 0, & \text{if } f > f_{\max} \\ \frac{(1-p_h)(f_{\max}-f)p_m}{f_{\max}-f_{db}^{up}}, & \text{if } f_{db}^{up} < f \leq f_{\max} \\ (1-p_h)p_m, & \text{if } f_{db}^{lo} < f \leq f_{db}^{up} \\ p_m - \frac{p_h(f-f_{\min})p_m}{f_{db}^{lo}-f_{\min}}, & \text{if } f_{\min} < f \leq f_{db}^{lo} \\ p_m, & \text{if } f \leq f_{\min} \end{cases} \quad (12)$$

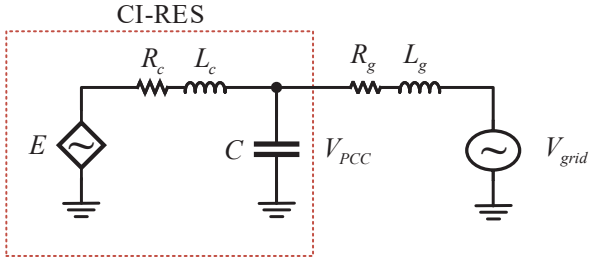


Fig. 2. Single-phase equivalent model of a CI-RES connected to the grid.

TABLE I
MODEL AND GRID PARAMETERS

Parameter	Value	Parameter	Value	Parameter	Value
L_c	1.5 mH	L_g	0.5 mH	p_h	0.2
R_c	0.03 Ω	R_g	0.03 Ω	f_{\min}	49 Hz
C	15 μF	V_r	400 V	f_{\max}	51 Hz
S_r	20 kVA	f_r	50 Hz	f_{db}	0.4 Hz
H	5 s	k_i^v	4e-5		

where f is the grid frequency that can be indirectly measured using ω in the proposed model, p_m is the maximum power available from the primary source of the CI-RES, and p_h is the power devoted to the PFR. Furthermore, f_{db}^{up} and f_{db}^{lo} are the upper and lower frequency deadbands which are equal $f_r + 0.5f_{db}$ and $f_r - 0.5f_{db}$, where f_r denotes the nominal grid frequency. In case the grid frequency lies outside f_{db}^{up} and f_{db}^{lo} , PFR is activated. Finally, f_{\min} and f_{\max} are the minimum and maximum frequency limits for the provision of PFR.

V. NUMERICAL RESULTS

The performance of the proposed model is evaluated by performing time-domain simulations and stability analysis assuming the configuration depicted in Fig. 2. The model and the network parameters are presented in Table I.

Initially, the grid voltage and frequency are equal to the nominal values V_r and f_r shown in Table I. The PFR is deactivated and the CI-RES injects active and reactive power to grid equal to 0.225 pu and 0.25 pu, respectively. At 0.5 s, a frequency event occurs and the grid frequency decreases with a rate of change of frequency (ROCOF) equal to 1 Hz/s till 1.5 s. The output power of the proposed model is presented in Fig. 3 and compared against the solution proposed in [9] assuming different values of D_p . According to Fig. 3a, it can be concluded that the proposed model provides a close to ideal IR, while maintaining a critically damped system. Furthermore, the proposed model effectively decouples the RPCL from the APCL, as shown in Fig. 3b. On the contrary, in the approach proposed in [9], the introduction of the damping term in the magnitude of the internal voltage strongly affects the reactive power output, as verified in Fig. 3b. Moreover, the overshoot in the IR cannot be fully eliminated since a further increase of D_p would result in model instability.

Afterward, the simulation is repeated assuming various combinations for the provision of IR and PFR, as shown in Fig. 4a. Considering the combined provision of IR and PFR, the following two scenarios are examined: (a) simultaneous

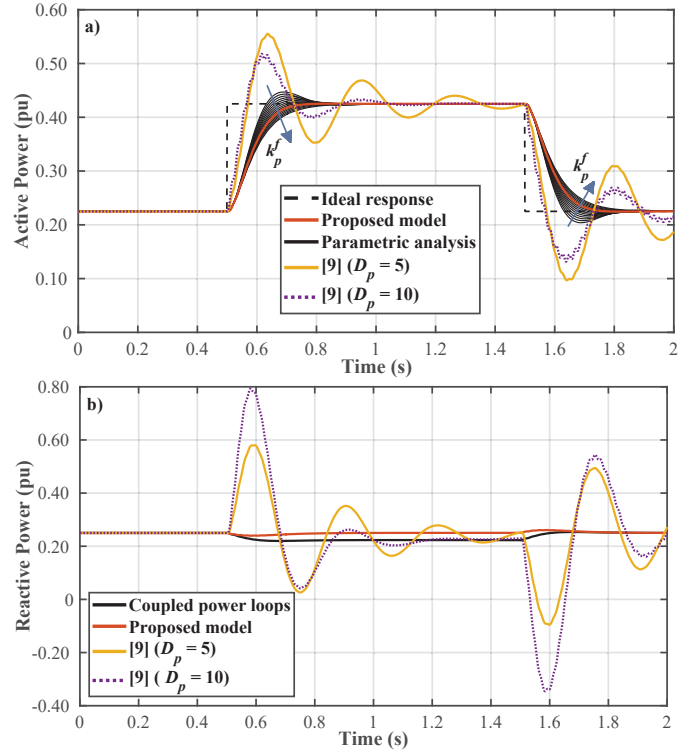


Fig. 3. CI-DRES output power. a) Active power and b) reactive power.

provision and (b) sequential provision. Note that in all cases, p_m is equal to 0.75 pu. It can be observed that the proposed model presents a well-damped behavior in all the examined scenarios. Moreover, IR is fully decoupled from PFR, allowing their distinct handling. On the contrary, in both versions of the synchronverter model proposed in [2] and [7], the oscillations are poorly damped, as verified in Fig. 4b. Furthermore, by increasing D_p , the damping of the system is improved at the expense of the PFR provision, highlighting a strong coupling between damping of oscillations and PFR. Finally, the most critical eigenvalues of both models are displayed in Fig. 5. It can be seen that the eigenvalue of the synchronverter model is located at the poorly damped region with a damping ratio (ζ) equal to 0.86 %. On the contrary, the dynamic response of the proposed model is well-damped by moving this eigenvalue to the real axis.

VI. CONCLUSIONS

In this short communication, an improved version of the synchronverter model is proposed. The distinct advantages of the proposed model are the following: (a) improved damping, (b) decoupled power loops, and (c) distinct handling of IR and PFR. Moreover, a condition for critically damped system is presented. The validity of the proposed model is assessed by performing time-domain simulations, revealing its improved performance compared to the synchronverter model.

REFERENCES

- [1] H. Gu, R. Yan, and T. K. Saha, "Minimum synchronous inertia requirement of renewable power systems," *IEEE Trans. Power Syst.*, vol. 33, no. 2, pp. 1533–1543, 2018.
- [2] Q. Zhong and G. Weiss, "Synchronverters: Inverters that mimic synchronous generators," *IEEE Trans. Ind. Electron.*, vol. 58, no. 4, pp. 1259–1267, 2011.

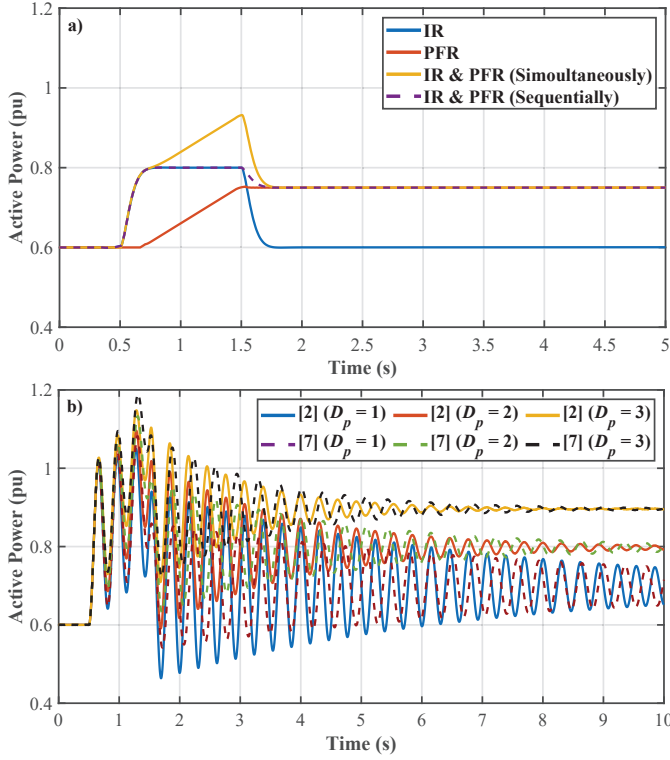


Fig. 4. CI-DRES active power. a) Proposed model and b) two versions of the synchronverter.

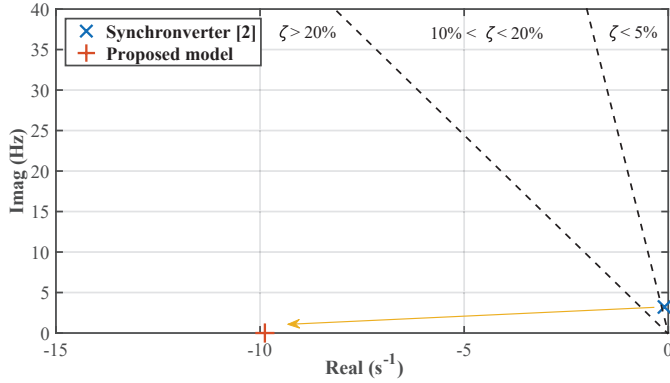


Fig. 5. Dominant eigenvalue.

- [3] ENTSO-E, "Frequency sensitive mode: Guidance document for national implementation for network codes on grid connection," pp. 1–13, 2018.
- [4] D. Li, Q. Zhu, S. Lin, and X. Y. Bian, "A self-adaptive inertia and damping combination control of VSG to support frequency stability," *IEEE Trans. Energy Conv.*, vol. 32, no. 1, pp. 397–398, 2017.
- [5] U. Markovic, N. Früh, P. Aristidou, and G. Hug, "Interval-based adaptive inertia and damping control of a virtual synchronous machine," in *2019 IEEE Milan PowerTech*, 2019, pp. 1–6.
- [6] U. Markovic, Z. Chu, P. Aristidou, and G. Hug, "Lqr-based adaptive virtual synchronous machine for power systems with high inverter penetration," *IEEE Trans. Sustain. Energy*, vol. 10, no. 3, pp. 1501–1512, 2019.
- [7] V. Natarajan and G. Weiss, "Synchronverters with better stability due to virtual inductors, virtual capacitors, and anti-windup," *IEEE Trans. Ind. Electron.*, vol. 64, no. 7, pp. 5994–6004, 2017.
- [8] Q. Zhong, G. C. Konstantopoulos, B. Ren, and M. Krstic, "Improved synchronverters with bounded frequency and voltage for smart grid integration," *IEEE Trans. Smart Grid*, vol. 9, no. 2, pp. 786–796, 2018.
- [9] M. Ebrahimi, S. A. Khajehoddin, and M. Karimi-Ghartemani, "An improved damping method for virtual synchronous machines," *IEEE Trans. Sustain. Energy*, vol. 10, no. 3, pp. 1491–1500, 2019.
- [10] S. D'Arco, J. A. Suul, and O. B. Fosso, "A virtual synchronous machine implementation for distributed control of power converters in smartgrids," *Electr. Power Syst. Res.*, vol. 122, pp. 180–197, 2015.